Analytical Biochemistry 529 (2017) 30–39

Contents lists available at ScienceDirect

Analytical Biochemistry

journal homepage: www.elsevier.com/locate/yabio

A practical guide to *in vivo* proton magnetic resonance spectroscopy at high magnetic fields

Lijing Xin [a, *], Ivan Tkáč [b, **]

[a] Animal Imaging and Technology Core (AIT), Center for Biomedical Imaging (CIBM), Ecole Polytechnique Fédérale de Lausanne, Lausanne, Switzerland
[b] Center for Magnetic Resonance Research, University of Minnesota, Minneapolis, MN, USA

ARTICLE INFO

Article history:
Received 13 August 2016
Received in revised form
3 October 2016
Accepted 19 October 2016
Available online 20 October 2016

Keywords:
MRS
Localization
Spectral quality
Brain
Metabolites

ABSTRACT

Localized proton magnetic resonance spectroscopy (^{1}H-MRS) is a noninvasive tool for measuring *in vivo* neurochemical information in animal and human brains. With the increase of magnetic field strength, whereas localized ^{1}H-MRS benefits from higher sensitivity and spectral dispersion, it is challenged by increased spatial inhomogeneity of the B_0 and B_1 fields, larger chemical shift displacement error, and shortened T_2 relaxation times of metabolites. Advanced localized ^{1}H-MRS methodologies developed for high magnetic fields have shown promising results and allow the measurement of neurochemical profiles with up to 19 brain metabolites, including less-abundant metabolites, such as glutathione, glycine, γ-aminobutyric acid and ascorbate. To provide a practical guide for conducting *in vivo* ^{1}H-MRS studies at high magnetic field strength, we reviewed various essential technical aspects from data acquisition (hardware requirements, B_1 and B_0 inhomogeneity, water suppression, localization sequences and acquisition strategies) to data processing (frequency and phase correction, spectral quality control, spectral fitting and concentration referencing). Additionally, we proposed guidelines for choosing the most appropriate data acquisition and processing approaches to maximize the achievable neurochemical information.

© 2016 Elsevier Inc. All rights reserved.

Introduction

Proton magnetic resonance spectroscopy (^{1}H-MRS) is widely used to noninvasively investigate biochemical information from selected regions in human and animal brains. This unique feature of ^{1}H-MRS is based on its spatial localization capability, i.e. providing spectra from selected volumes of interests (VOI), which is the biggest difference from high-resolution ^{1}H NMR spectroscopy of liquids commonly used in bio-, analytical or organic chemistry. The advantage of ^{1}H-MRS originates from the highest sensitivity of protons relative to other nuclei because of their nearly 100% natural abundance and high gyromagnetic ratio. The sensitivity further increases with the magnetic field strength (B_0) that is also beneficial for improved spectral resolution due to increased chemical shift dispersion. However, at higher B_0 fields the localization becomes more challenging due to spatial inhomogeneity of the radiofrequency transmit field (B_1) and larger chemical shift displacement errors (CSDE). In addition, the spectral resolution is challenged by shortened T_2 relaxation times of metabolites and increased inhomogeneity of the B_0 field. Advanced ^{1}H-MRS methodologies (including B_0 shimming, localization sequences, water suppression, processing and quantification) developed for high magnetic fields have shown very promising results [1–4]. These techniques provide neurochemical profiles with up to 19 brain metabolites, including uncommon and less-abundant metabolites, such as glutathione (GSH) [5,6], glycine (Gly) [7] and ascorbate (Asc) [8]. In addition, these techniques provide improved separation of metabolites with similar ^{1}H-MR spectra (e.g. glutamate and glutamine) [9–13]. The potential of high-field ^{1}H-MRS has been nicely demonstrated by the ability to detect very small metabolic changes in the brain induced by different types of physiological stimulations [14–17]. These advanced ^{1}H-MRS techniques have been successfully applied in many clinical and preclinical studies that focused on cerebral metabolic alterations in neurological disorders, psychiatric and neurodegeneration diseases, stroke and

* Corresponding author. Centre d'Imagerie BioMédicale (CIBM), Ecole Polytechnique Fédérale de Lausanne (EPFL), EPFL-SB-CIBM-AIT, Station 6, CH-1015, Lausanne, Switzerland.
** Corresponding author. Center for MR Research, Department of Radiology, University of Minnesota, 2021 6th St. S.E., Minneapolis, MN 55455, USA.
E-mail addresses: lijing.xin@epfl.ch (L. Xin), ivan@cmrr.umn.edu (I. Tkáč).

http://dx.doi.org/10.1016/j.ab.2016.10.019
0003-2697/© 2016 Elsevier Inc. All rights reserved.

brain cancer [18–22]. These studies provided a better understanding of the pathogenesis of these diseases on a molecular level and led to improvements in diagnosis, disease monitoring and treatment assessment.

Excellent localization performance is a key prerequisite for reliable metabolite quantification. Here we review the technical aspects of *in vivo* ^{1}H-MRS from data acquisition (hardware requirements, B_1 and B_0 homogeneity, water suppression, localization sequences and acquisition strategies) to data processing (frequency and phase correction, spectral quality control, spectral fitting and concentration referencing) at high magnetic field strength (above 3 T for humans and above 7 T for animals). In addition, we provide guidelines for choosing the most appropriate data acquisition and processing approaches in order to maximize the neurochemical information that can be potentially achieved.

Data acquisition

Hardware requirements

Magnets are the most essential part of all MRI scanners. Powerful magnets are highly preferential for MRS because of their increased sensitivity for detecting brain metabolites, whose concentrations are three to four orders of magnitude lower than that of water. However, wide-bore magnets for human body MRI/MRS are substantially more complex and expensive than the narrow bore magnets used for high-resolution NMR spectroscopy of liquids. Consequently, 7 T MR scanners are currently considered ultra-high field systems and are used only for research applications on humans. However, for clinical MRS applications, 3 T is currently the highest field. MR scanners equipped with 9.4T and 11.7T horizontal magnets (bore size = 16–30 cm) currently seem to be the best compromise between cost and performance for small animal (mice, rats) MRI/MRS.

Even though the latest high-field models from all major MRI vendors meet the basic hardware requirements for MRS, this technique has specifically high demands on the radiofrequency (RF) transmit system (RF amplifiers, RF coils) and the 2nd-order shim system for adjustment of the B_0 field homogeneity (1st-order shims are always strong enough because the main gradient coils and gradient amplifiers are used for this purpose). A proper hardware configuration of the RF transmit chain is particularly important for human brain MRS at 7 T where the wavelength of the RF field becomes comparable to the size of the head. This phenomenon results in destructive interferences between B_1^+ fields transmitted by the individual elements of the RF coil causing a major spatial non-uniformity of the transmit B_1^+ field. In addition, achieving sufficiently strong B_1^+ at 7 T is challenged by an increased power deposition (specific absorption rate, SAR) at high fields, which may potentially lead to tissue overheating. Technically it is much easier to generate sufficiently high transmit B_1^+ with the small RF coils used for MRI/MRS in rodents. For brain spectroscopy of mice or rats, we recommend the use of transmit/receive quadrature surface RF coils with two geometrically decoupled single-turn loops (10–20 mm diameter) because of their high detection sensitivity [10,23]. Another alternative is to use a combination of two RF coils, a volume coil for transmit and a small surface coil only to receive.

Precise adjustment of the static magnetic field homogeneity within the selected VOI, commonly known as B_0 shimming, is essential for ^{1}H-MRS because it directly affects the signal linewidth, which determines the spectral resolution, signal-to-noise ratio (SNR) and consequently the reliability of metabolite quantification. Since the B_0 field inhomogeneities become highly nonlinear at increased field strengths, a higher-order shim coil system is necessary to compensate them. However, across the small VOIs typically selected for regionally-specific ^{1}H-MRS, these inhomogeneities can be well approximated by 2nd-order functions. Therefore, a powerful 2nd-order shim system is usually sufficient for single-voxel ^{1}H-MRS. A powerful shim system requires suitable shim coils and shim coil drivers to generate B_0 fields of appropriate symmetry and strength. The strength of the 2nd-order shims on human 7T MRI scanners should be at least 30 Hz/cm^2 (0.7 μT/cm^2) for XZ, YZ and Z2 and 15 Hz/cm^2 (0.3 μT/cm^2) for XY and X2Y2 shims [3]. On animal 9.4T MRI scanners, these values have to be at least 2000 Hz/cm^2 (47 μT/cm^2) for XZ, YZ and Z2 and 1000 Hz/cm^2 (23.5 μT/cm^2) for XY and X2Y2 [4]. Requirements for higher B_0 fields can be estimated by scaling these values by the field strength.

Transmit B_1^+ field management

The requirements for a maximum transmit B_1^+ field increase linearly with main magnetic field strength B_0 because of the demands for broadband RF pulses to minimize unwanted CSDE at high fields (explained in Section Localization techniques). Therefore, human 7T MRI scanners are typically equipped with multichannel transmit systems with at least 8 kW total output power feeding surface, quadrature half-volume or volume RF coils. These surface or quadrature half-volume RF coils are capable of providing sufficiently strong peak B_1^+ field (on the order of 40–50 μT), but only in relatively close proximity of the RF coil. However, achieving sufficiently high transmit B_1^+ field in any brain region becomes challenging at higher fields when using a volume RF coil. Destructive interferences cause an inhomogeneous B_1^+ distribution and when combined with the pattern of the receive B_1^- field they lead to high sensitivity in the middle of the head and low sensitivity in the periphery [24].

Several approaches have been proposed to improve B_1^+ efficiency in the region of interest: 1) using a multi-channel transmit system to control the amplitudes and phases of individual coil elements to maximize transmit B_1^+ field in the selected VOI, so called RF shimming [24–26]; 2) designing multidimensional RF pulses [27–29], and 3) placing a pad with high dieletric material [30,31] close to the head. Although RF shimming has been successfully demonstrated for single voxel ^{1}H-MRS [32], the complex hardware and software requirements still limit its application. The use of a dieletric pad is the simplest approach and has been shown to maximize the transmit B_1^+ field in the medial temporal lobe [30], parietal lobe (Fig. 1) [17] and prefrontal lobe (unpublished data). Deuterated water is recommended as the solvent for dielectric materials to reduce a possible interference between the solvent signal and metabolite signals from the VOI (water resonance from the dielectric pad is significantly shifted relative to the brain water resonance).

B_0 shimming

Abovementioned hardware requirements (shim coils and drivers) are necessary but not sufficient for successful B_0 shimming. First, the B_0 field inhomogeneity over the region of interest must be precisely measured using an appropriate B_0 mapping method. These methods are based either on 3D B_0 mapping [33] or mapping along projections [34–36]. Both approaches use the phase difference acquired during the free precession of the magnetization in an inhomogeneous B_0 field to calculate the field distribution. The 3D B_0 mapping methods are adequate for global B_0 shimming in MRI. However, for a very fine adjustment of the field, which is essential for single-voxel MRS, these techniques are often outperformed by projection techniques, such as FASTMAP [34]. This method is based on a sparse, yet efficient sampling of the magnetic field along a

Fig. 1. Example of improved local transmit B_1^+ field in the motor cortex using a dielectric pad containing a solution of deuterated water and barium titanate (dielectric permittivity of 160) (red bar in the middle image). Experimental B_1^+ field maps without (left) and with (middle) the dielectric pad present. The ratio of the two images (right) shows a B_1^+ increase by a factor of two in the motor cortex, above which the pad was placed. The scale of the B_1^+ maps, obtained using the SA2RAGE (SAturation-prepared with 2 RApid Gradient Echoes) sequence [71] (TR = 2400 ms, TE = 0.78 ms, TD_1 = 45 ms, TD_2 = 1800 ms, $\alpha 1 = 4°$, $\alpha 2 = 10°$, 2 × 2 × 2.5 mm^3 resolution and a 128 × 128 × 64 matrix size acquired with sagittal orientation, TA = 1 min 55 s, reference voltage = 170 V) corresponds to a multiplicative factor of a desired flip angle (Adapted from Ref. [17], with permission from Elsevier).

limited number of projections (3 for linear and 6 for 2nd-order shims), which effectively accelerates the data collection. In addition, 1D projections can easily provide field mapping data with high spatial resolution, which is essential for precise adjustment of the field homogeneity in the small volumes typical for single voxel MRS. Here we explain how the spatial resolution of mapping and the phase evolution delay affect the outcome of the B_0 shimming. First, there must be enough points in all three spatial directions within the shimmed region to do meaningful polynomial analysis. Secondly, short evolution delays are necessary to avoid phase wrapping when the B_0 field inhomogeneity is poor, but such short delays make the mapping insensitive for small B_0 variations. Therefore, long evolution delays are necessary for the fine adjustment of the B_0 homogeneity. These problems can be easily solved by a multi-echo mapping approach, such as FASTMAP with EPI readout [35], where short and long evolution delays are acquired simultaneously. It is important to keep in mind that proper B_0 shimming always requires a 3D volume of a reasonable size despite the shape of the VOI, which might be relatively flat. The *in vivo* ^{1}H-MR spectra shown in Fig. 2 illustrate the spectral resolution achievable in the human brain at 7 T [2] and in the animal brain at 9.4T when the local B_0 field homogeneity is well adjusted. For more details about B_0 shimming, see the paper by Juchem & de Graaf in this special issue.

Water suppression

For *in vivo* ^{1}H MR spectroscopy, the signal intensity of protons in water molecules, which resonate around 4.7 ppm is about three to four orders of magnitude higher than the intensities of metabolite spectra and the water signal's broad shoulders overlap with resonances of interest if not suppressed. This huge water signal does not only cause baseline distortions, but it also contains spurious satellites from mechanical vibrations of the gradient coil that overlap with the spectra of metabolites. Therefore a water suppression module is nearly always included in ^{1}H MR spectroscopic sequences to simplify the spectral quantification.

The different physical properties of water and metabolites, such as differences in chemical shift and relaxation times, can be exploited for a selective removal of the water peak. Under *in vivo* conditions, the water protons resonate at ~4.7 ppm, while most metabolites resonances can be found either <4.2 ppm or >5.2 ppm. Therefore, frequency-selective, narrow-band RF pulses are required to target the water resonance without affecting metabolites of interest. Chemical shift selective (CHESS) water suppression [37] is commonly used, which consists of a narrow-band, frequency-selective excitation followed by magnetic field gradients that dephase the transverse magnetization of water.

Efficient water suppression is challenging in the presence of an inhomogeneous transmit B_1^+ field produced by surface RF coils. In addition, water signal originates from different compartments within the brain (gray and white matter, cerebrospinal fluid) with different T_1 relaxation times, which makes the suppression even more challenging. The combination of multiple CHESS elements with optimized RF pulse flip angles (WET [38] and VAPOR [3,10]) decreases the sensitivity on RF power adjustment, improving the robustness of the water suppression. The VAPOR (VAriable Pulse power and Optimized Relaxation delays) scheme using seven or eight CHESS elements with optimized inter-pulse delays routinely provides highly efficient water suppression, leaving a residual water signal well below the intensity of major brain metabolites (Fig. 3). The robustness of VAPOR water suppression allows for an automatic setting of all its parameters (including the RF power) that helps to reduce the time necessary to optimize pulse sequence parameters for the chosen VOI. The bandwidth of water suppression RF pulses (in Hz) must be set according to the B_0 field strength to keep the chemical shift selectivity in a reasonable range (4.2–5.2 ppm), which allows the detection of signal from H-1 proton of α-glucose at 5.23 ppm (Fig. 3c). This frequency selectivity of the water suppression is improved at ultra-high fields due to increased chemical shift dispersion, as the spectral range of 4.2–5.2 ppm on a Hz scale is proportional to the B_0 field (e.g. it

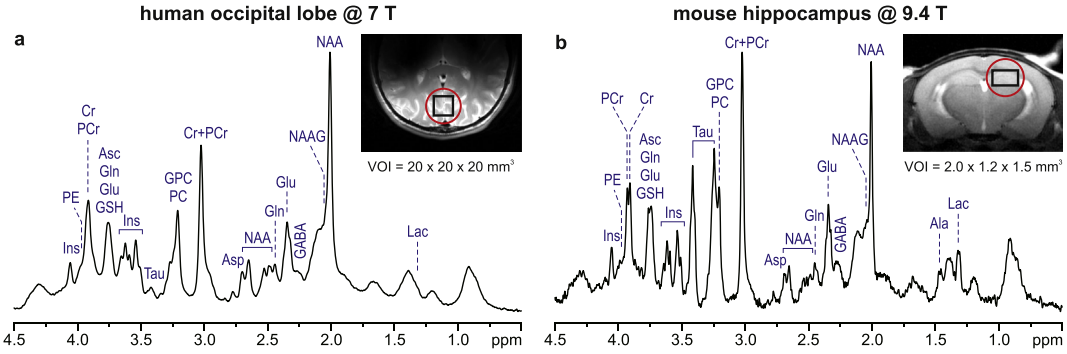

Fig. 2. Examples of the spectral resolution achievable in ^{1}H MR spectra acquired from human and animal brains with optimal B_0 shimming. (a) Gray-matter-rich occipital lobe of a human subject (STEAM, B_0 = 7 T, TE = 6 ms, VOI = 8 ml); (b) mouse hippocampus (STEAM, B_0 = 9.4 T, TE = 2 ms, VOI = 3.6 μl). Red circles around the VOIs illustrate the volume prescribed for local B_0 shimming using FASTMAP.

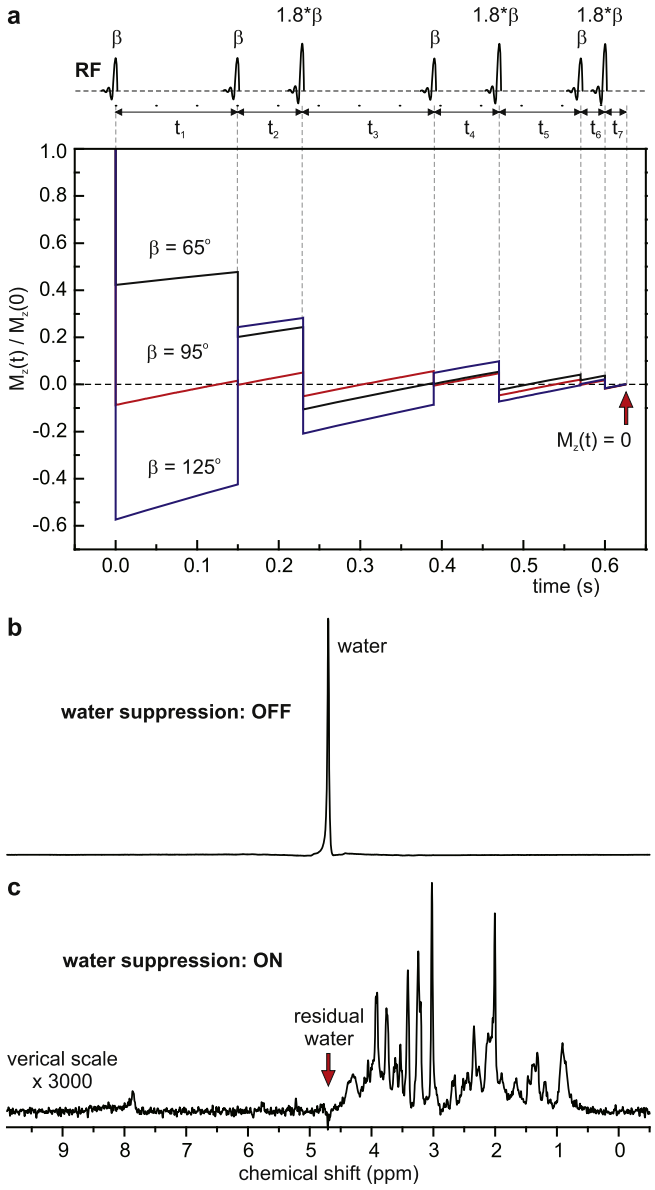

Fig. 3. (a) Simplified diagram of the VAPOR water suppression and time dependences of the water longitudinal magnetization (M_z) calculated for three different values of the nominal flip angle (65°, 95° and 125°), assuming a water relaxation time T_1 of 1.5 s [10]. Using optimized time delays (150 ms, 80 ms, 160 ms, 80 ms, 100 ms, 30 ms and 26 ms for delays t_1 to t_7, respectively), the residual M_z of water protons reaches zero at the end of t_7. *In vivo* ^{1}H MR spectra of the mouse brain acquired with the VAPOR water suppression OFF (b) and ON (c). STEAM, TE = 2 ms. The VAPOR diagram (a) modified with permission from Tkac et al. [10] 1999 © John Wiley and Sons.

corresponds only to 128 Hz at 3 T, but to 300 Hz at 7 T). The bandwidth and the profile of the RF pulses must be wide enough to suppress the water signal even outside of the VOI, where the water resonance frequency could be considerably shifted due to B_0 inhomogeneity. At the same time, the selectivity of these RF pulses must be high enough to guarantee that metabolite resonances near the water resonance are not affected. Therefore, we suggest that using RF pulses with flat excitation profiles, whose saturation effect outside of a ±0.5 ppm range does not exceed 5%, is a reasonable compromise. Spurious echoes, originating from brain regions distant from the selected VOI where the water resonance is shifted outside of the water suppression pulse BW, can be efficiently suppressed by outer volume suppression (introduced in the next section).

Localization techniques

Volume selection is a fundamental attribute of single-voxel MRS. Spatial localization is typically achieved by a combination of three orthogonal slice-selective pulses that use the simultaneous application of a frequency selective RF pulse together with a magnetic field gradient (G). The resulting slice thickness is defined as $2\pi.BW/\gamma G$, where BW is the bandwidth of the applied RF pulse and γ is the gyromagnetic ratio of protons. However, this volume is precisely selected only for spins whose resonance frequency is equal to the carrier frequency of the applied RF pulses. Metabolite resonances actually experience different excitation volumes due to off-resonance effects resulting from their difference in chemical shifts. The shift of the excitation volume relative to the prescribed volume is called chemical shift displacement error (CSDE), which is defined as $\Delta\nu/BW$ where $\Delta\nu$ is the frequency difference of a particular resonance from a chosen carrier frequency. With the increase of magnetic field strength, the chemical shift dispersion is linearly enlarged, e.g. the separation of lactate (CH_3 group) at 1.3 ppm and creatine (CH_2 group) at 3.9 ppm increases from 334 Hz at 3 T to 780 Hz at 7 T, which in turn leads to a larger CSDE. In order to reduce this unwanted CSDE and improve the localization performance, broadband RF pulses and correspondingly larger gradient strengths are required for high-field MRS. Some common localization strategies developed for high fields include: outer volume suppression, and STEAM [2,10], SPECIAL [5,39,40] and semi-LASER pulse sequences [41,42], which are explained in more detail in the following sections.

Outer volume suppression

Outer volume suppression (OVS) is a localization technique that suppresses the signal from outside the VOI without perturbing the magnetization inside the VOI [43,44]. Specifically, slice-selective pulses are used to excite the magnetization outside of the VOI, which is immediately dephased by crusher gradients. Localization of a 3D volume commonly requires six OVS slabs around the VOI. To acquire the signal from the VOI, a nonselective RF pulse can be applied following the OVS block. Since the magnetization inside the VOI is not perturbed, there is no signal loss due to relaxation, which makes OVS a suitable scheme for acquiring spectra of molecules with very short T_2 relaxation times. CSDE of the OVS can be reduced by using broadband adiabatic RF pulses, such as a hyperbolic-secant pulse (Fig. 4a) [3]. The OVS block can be repeated multiple times with variable transmit B_1^+ peak amplitudes to improve the efficiency of OVS when the transmit B_1^+ field is spatially inhomogeneous [3]. In addition, the OVS scheme can be combined with other localization sequences to further improve the efficiency of the localization and to reduce the demand for crusher gradients that dephase unwanted coherences.

Ultra-short echo-time STEAM sequence

The STEAM (Stimulated Echo Acquisition Mode) sequence [45], which consists of three consecutive 90° frequency selective RF pulses applied in the presence of orthogonal slice selection gradients generate a stimulated echo from a 3D volume (Fig. 4b). Crusher gradients during echo-time (TE) and mixing-time (TM) periods are set to dephase all unwanted coherences from outside and also inside of the VOI. Asymmetric 90° RF pulses can be advantageously used in the STEAM sequence to achieve a TE as short as 1 ms in small animal studies at 9.4 T [10] or 6 ms in human applications at 7 T [2]. Using an ultra-short TE is extremely beneficial for absolute

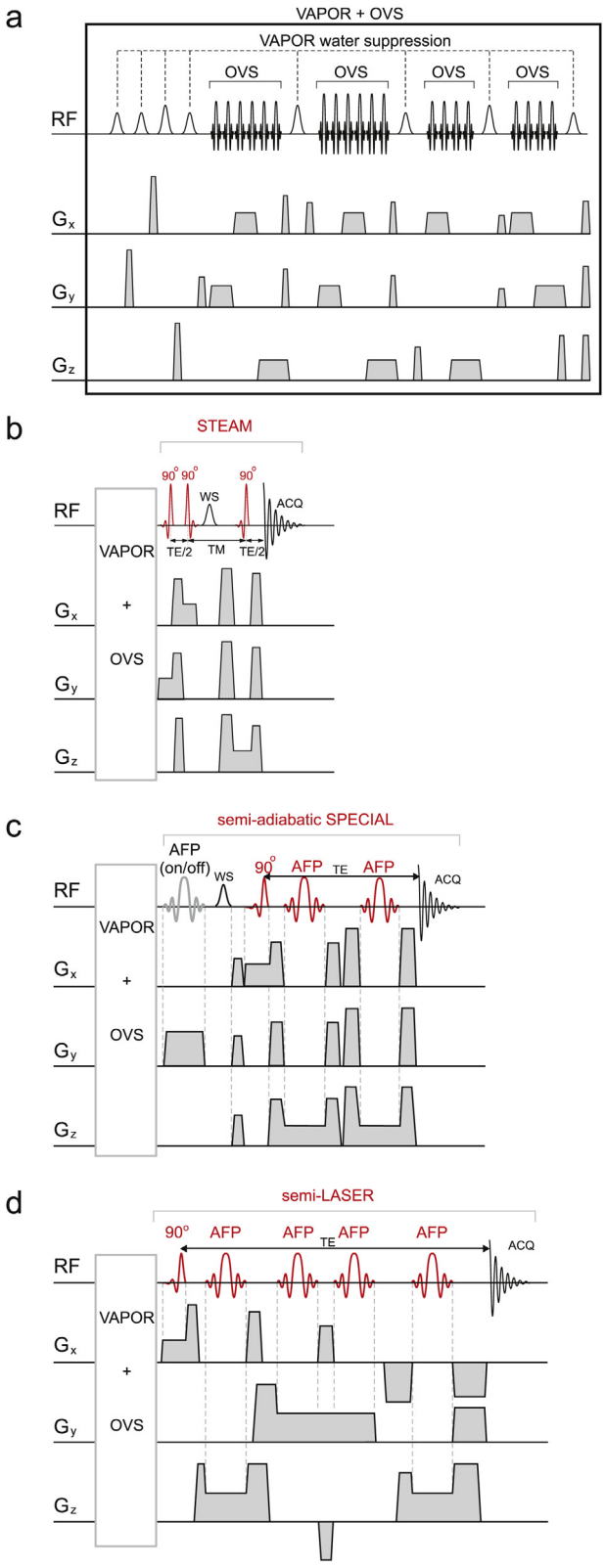

Fig. 4. A schematic drawing of the outer volume suppression (OVS) interleaved with the VAPOR water suppression (a). Pulse sequence diagrams of STEAM (b), semi-adiabatic SPECIAL (c) and semi-LASER (d) for short echo-time *in vivo* ^{1}H MRS at high magnetic fields.

metabolite quantification because T_2 relaxation effects can be neglected. In addition, using these 90° RF pulses for human head studies at 7 T enables the increase of the bandwidth up to 4.5 kHz despite limitations on the maximum available transmit B_1^+ field, which is often below 25 μT ($\gamma B_1/2\pi = 1.1$ kHz) [10]. Such a bandwidth keeps the CSDE in a reasonable range below 20% of the voxel size (for lactate signal at 1.3 ppm and creatine signal at 3.9 ppm) along each gradient direction. Moreover, additional water suppression RF pulse can be applied during the TM period for final elimination of the residual water signal. The main disadvantage of the STEAM sequence is the fact that it provides less signal than other spin-echo based pulse sequences (e.g. semi-LASER, SPECIAL) because it uses only half of the available M_z magnetization (the second half is dephased during the TM period). Another drawback of the STEAM sequence with an ultra-short TE is an increased signal contribution from fast-relaxing macromolecules that makes the metabolite quantification more challenging, especially for weakly represented metabolites, such as γ-aminobutyric acid.

Semi-adiabatic SPECIAL sequence

The spin-echo full-intensity acquired localized spectroscopy (SPECIAL) sequence [5,39] combines two different spatial localization approaches, one-dimensional (1D) ISIS (image selected *in vivo* spectroscopy [46]) and 2D spin-echo based localization. The 1D ISIS localization is achieved by applying a slice-selective inversion using an adiabatic full-passage (AFP) RF pulse on alternate scans. This type of localization requires adding or subtracting alternating scans to separate the signal originating only from the selected slice. The original implementation of the SPECIAL sequence on 7 T used an asymmetric 90° pulse and amplitude modulated refocusing pulse in the spin-echo part that allowed that the TE be reduced to 5.5 ms [5]. However, due to a maximum available transmit B_1^+ field below 40 μT, the bandwidth of the 180° refocusing RF pulse was only 1.8 kHz, which led to a CSDE over 40%. In order to minimize this hardly acceptable CSDE, this amplitude-modulated refocusing RF pulse was replaced by a pair of broadband AFP pulses (BW = 7.4 kHz) [47] that reduced the CSDE to 11%. Consequently, the minimum TE of this version of the sequence, called semi-adiabatic SPECIAL [40] (Fig. 4c), increased to 12 ms for a surface coil and 16 ms for a birdcage coil. The semi-adiabatic SPECIAL sequence and the STEAM sequence are the methods of choice for ultra-short TEs. The main advantage of the SPECIAL sequence relative to STEAM is the fact that it provides full signal intensity for the selected VOI. However, the SPECIAL sequence is not a single-shot technique and its add-subtract scheme can lead to subtraction artifacts because of physiological or subject motion.

LASER and semi-LASER sequences

The LASER (Localization by Adiabatic SElective Refocusing) sequence is a single-shot full-intensity technique [48], where the volume selection is accomplished by three pairs of AFP pulses. Since the spins are excited by a preceding adiabatic RF pulse (half-passage), the whole localization sequence is adiabatic, which is highly beneficial for experiments using surface or half-volume RF coils with spatially inhomogeneous transmit B_1^+ field. When the maximum available B_1^+ is high enough, as it commonly is for the small RF coils used in rodent studies, a minimum TE of 15 ms is feasible [23]. However, the maximum B_1^+ field available on human MR scanners is much lower, which is especially true for 3T scanners equipped with a body transmit RF coil. Accordingly, LASER's six AFP pulses must be much longer, which considerably prolongs the minimum TE [49] and complicates metabolite quantification due to T_2 relaxation and J-evolution effects. This disadvantage of the LASER sequence can be reduced by substituting the excitation RF pulse and one pair of AFP pulses for a non-adiabatic slice-selective excitation. This version of the localization pulse sequence is no

longer fully adiabatic and therefore, the acronym semi-LASER or sLASER was created for this technique [41,42].

The semi-LASER localization technique (Fig. 4d) allows the shortest TE to be below 30 ms for different MRI scanner hardware configurations from 3 to 7 T [6,42]. In this sequence, an asymmetric 90° pulse is combined with two pairs of broadband AFP pulses and corresponding slice-selection gradients select a 3D volume with reasonably low CSDE (17% along the direction selected by the 90° pulse and only 11% along the directions selected by the AFP pulses). A pair of AFP pulses is necessary for each slice orientation in order to compensate the quadratic phase shift across the slice that is induced by a single AFP pulse. It was demonstrated that all unwanted coherences can be eliminated in a single scan by an appropriate adjustment of crusher gradients [42]. Artifact free single scan data enable the use of a single scan averaging mode (explained in the next paragraph) that makes this localization sequence highly advantageous for patient studies when subject motion is anticipated (e.g. pediatrics, neurodegenerative diseases accompanied with involuntary movements) or for highly sensitive studies investigating metabolic changes during brain activation. While the shortest allowable TE of the semi-LASER sequence is longer than that of aforementioned sequences, the fast repetition of the AFP pulses reduces adverse effects of longer TE, i.e., it prolongs the apparent T_2 relaxation times of metabolites relative to those measured by a spin echo and partially suppresses the J-modulation in the spectra of metabolites with coupled spin systems.

Data acquisition

As previously mentioned, successful B_0 shimming is essential in order to maximize the spectral resolution. However, this condition is not sufficient for achieving the best spectral resolution obtainable. Physiological motion (respiratory and cardiac cycles), small head motions or hardware instability (B_0 field drift) during data collection may induce frequency and phase fluctuations that result in substantial spectral quality deterioration if uncorrected. Therefore, a single scan averaging mode during data collection, where each individual scan is stored separately, is preferential for *in vivo* applications because it allows for frequency and phase correction of individual scans before summation. If the SNR of a single scan is not sufficient for these types of corrections then the data acquisition in small blocks, e.g. four of eight scans per block, is highly recommended.

Many rat and mouse models of human neurodegenerative diseases have been developed to investigate the pathogenesis of these diseases and to improve our understanding of the underlying pathophysiological processes on a molecular level. During *in vivo* ^{1}H-MRS experiments animals must be immobilized using appropriate anesthesia. In order to keep the animal under optimal physiological conditions while in the magnet, basic physiological parameters (at least body temperature and respiration rate) must be continuously monitored. It is highly recommended that the duration of the experiment not exceed two hours when spontaneous breathing of anesthetic gases (without active ventilation) is used. Keep in mind that suboptimal physiological conditions can not only change the concentrations of some brain metabolites, e.g. lactate (Lac) or the creatine to phosphocreatine ratio (Cr/PCr), but decreased oxygen saturation of blood also increases the spectral linewidth. Moreover, animal gasping causes major motion artifacts that cause phase fluctuations of the received signal. Animal holders should be designed to firmly keep the rat or mouse head from moving, but also minimize the time required to switch animals, which is important for increasing the throughput of ^{1}H-MRS methods. Good animal holders should not only allow for adjustment of the head position along the Z-axis (along magnet bore), but also enable rotation of the animal holder for easy and reproducible positioning of the animal head in the isocenter of the magnet [50].

Data processing and quantification

Data pre-processing

Single scan data averaging or data averaging in small blocks enables the correction of frequency and phase fluctuations before summation. In addition, if some scans or blocks are corrupted by hardware instability or animal motion, these data can easily be eliminated before summation, which helps to obtain the highest achievable spectral quality. The frequency and phase fluctuations can be assessed in the time or frequency domain, but these corrections have to be applied in the time domain (on free induction decays, FIDs) because the most frequently used metabolite quantification programs, such as jMRUI and LCModel (see Section Metabolite quantification) require data input in the time-domain. The next pre-processing step is the removal of residual eddy currents using unsuppressed water signal [51]. The extra benefit of this correction is the removal of signal satellites caused by gradient coil vibrations. Finally, it is beneficial to determine the absolute phase of the spectrum and use it later as a fitting input parameter in order to decrease the number of fitted variables.

Spectral quality

The primary goal of advanced ^{1}H-MRS is to maximize the neurochemical information that is possible to extract from the acquired spectra. Spectral quality is the most essential requirement for reliable quantification of a wide range of brain metabolites, the so-called “neurochemical profile”. Reasonably high SNR and superior spectral resolution are two important factors determining the spectral quality (Fig. 5). Reliable quantification, especially of weakly represented metabolites such as Asc, GABA, GSH or phosphoethanolamine (PE), also requires flat baseline, highly efficient water suppression and excellent localization performance. The localization performance of the sequence can easily be assessed from the spectral pattern between 0.5 and 1.8 ppm, which consists of four broad signals of fast relaxing macromolecules (MM). Any twist or deformation of this spectral pattern around 1.5 ppm indicates a spectral contamination by subcutaneous lipid signals from outside of the VOI (Fig. 5).

Metabolite quantification

Reliable non-invasive quantification of metabolites in a well-defined brain region is the ultimate goal of *in vivo* ^{1}H-MRS of the animal or human brain. Information about metabolite concentrations is extremely valuable for a better understanding of molecular mechanisms underlying normal brain function as well as molecular processes that lead to or accompany neurological disorders. In general, two steps are required for a meaningful quantification of metabolites. First, appropriate spectral fitting procedures have to be applied to decompose an acquired ^{1}H-MR spectrum into sub-spectra of brain metabolites. The second step is the normalization of these sub-spectra using a proper reference in order to estimate the concentrations of these metabolites.

Spectral fitting

Metabolites can be relatively easily quantified from high-resolution ^{1}H NMR spectra of biofluids by simple peak integration and line shape fitting. However, extracting meaningful information from *in vivo* ^{1}H MR brain spectra is rather complex even at ultra-high magnetic fields because of considerable overlap of

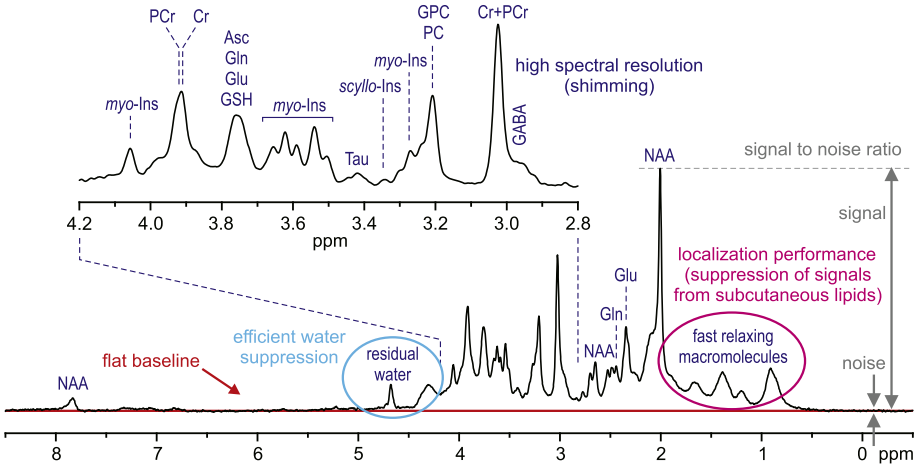

Fig. 5. Characteristic factors for *in vivo* ^{1}H-MR spectra quality assessment (STEAM, $B_0 = 7$ T, TE/TR = 6/5000 ms, VOI = 8 ml, number of transients (NT) = 160, gray-matter-rich occipital cortex). Modified with permission from McKay et al. [72] 2016 © Oxford Journals.

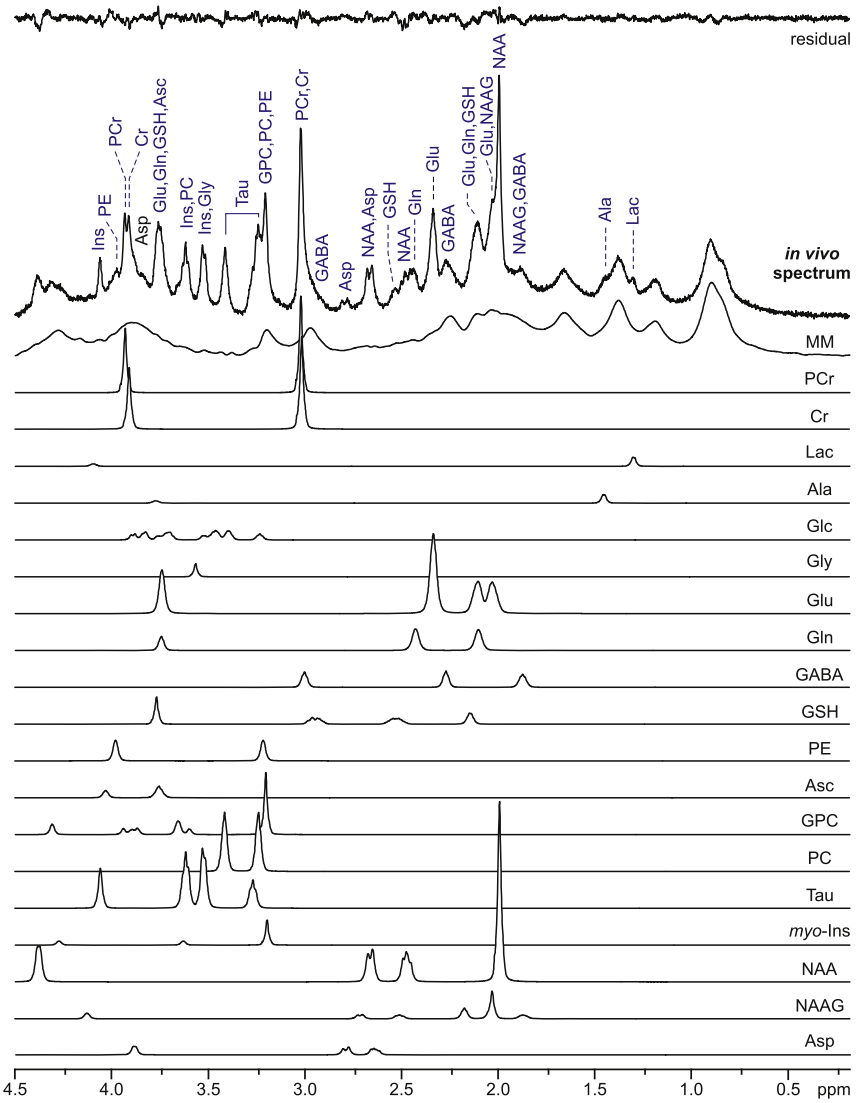

Fig. 6. The LCModel analysis of an *in vivo* ^{1}H MR spectrum acquired from a rat brain (SPECIAL, TE/TR = 2.8/4000 ms, NT = 240, VOI = 70 μl, frontal cortex, corpus callosum and striatum) at 14.1 T. The LCModel analysis shows the experimental *in vivo* spectrum, the fit residual, the spectra of individual metabolites and the spectrum of macromolecules included in the basis set. Used metabolite abbreviations: MM, macromolecules; PCr, phosphocreatine; Cr, creatine; Lac, lactate; Ala, alanine; Glc, glucose; Gly, glycine; Glu, glutamate; Gln, glutamine; GABA, γ-aminobutyric acid; GSH, glutathione; PE, phosphoethanolamine; Asc, ascorbate; GPC, glycerophosphocholine; PC, phosphocholine; Tau, taurine; *myo*-Ins, myo-inositol; NAA, N-acetylaspartate; NAAG, N-acetylaspartylglutamate; Asp, aspartate.

metabolite spectra, especially within the 1–4 ppm range, e.g. N-acetylaspartate (NAA), glutamate (Glu) and glutamine (Gln) (Fig. 6 top). Hence, sophisticated fitting procedures combined with extensive prior knowledge are required to obtain biochemically relevant information. Different fitting programs are available for ^{1}H-MRS data quantification: LCModel (Linear Combination of Model spectra) [52] that works in the frequency-domain or jMRUI (http://www.mrui.uab.es/mrui/) [53] and TARQUIN (Totally Automatic Robust QUantitation In NMR http://tarquin.sourceforge.net/user_guide/tarquin_user_guide.html) [54] in the time-domain.

The basic goal of LCModel analysis is to decompose an *in vivo* ^{1}H-MR spectrum into a linear combination of model spectra from the "basis set". The basis set is a database of metabolite spectra that dominantly contribute to an *in vivo* ^{1}H-MR spectrum of the brain. One straightforward way to generate a basis-set is to measure *in vitro* ^{1}H-MR spectra of all the individual metabolites in solution (pH = 7.2, T = 37 °C) under the same experimental condition (Larmor frequency, pulse sequence parameters). However, preparing metabolite solutions and scanning these samples is a tedious, time-consuming task and has to be repeated when the type of localization sequence or its parameters (e.g. TE) are changed or when the Larmor frequency is changed substantially (>0.5 MHz). As an alternative, the basis set can be simulated using the density matrix formalism and known chemical shift and J-coupling constants of brain metabolites [55]. The LCModel analysis provides the list of metabolite concentrations together with the Cramér-Rao lower bounds (CRLB), which are the estimates of the fitting errors, i.e. the statistical uncertainty of the concentration estimates [56]. These estimated errors are only appropriate if the model (basis set) is correct and complete [57]. This is obviously not possible, but reasonable simplifications have to be made to avoid any large-scale bias in metabolite quantification. An example of spectral fitting results obtained from LCModel analysis of a ^{1}H MR spectrum from a mouse brain is demonstrated in Fig. 6.

Reliable quantification of a wider range of metabolites from short echo-time ^{1}H-MR spectra is challenging because metabolite resonances not only overlap with each other, but also overlap with broad signals of fast relaxing (T_2) MM. The accurate modeling of MM signals is critical for the accurate estimates of metabolite concentrations [58]. The MM spectrum can be separated from low-molecular-weight metabolites based on differences in T_1 and T_2 relaxation times [59,60] and apparent diffusion coefficients [61]. Two approaches are commonly used to treat the broad underlying signals of MM in fitting procedures. These broad MM signals can be estimated by mathematical models, such as spline functions [52,62]. The second approach includes the experimentally measured MM spectrum, using inversion recovery [63,64] or diffusion weighted method [61], in the LCModel basis set. At low field strength $\leq$ 3T, the mathematically estimated MM contribution has shown a very similar spectral pattern as the experimentally measured MM spectrum and appears to be sufficient for accurate estimation of metabolite concentrations [63]. In addition, the flexibility of the mathematical estimation may be advantageous for dealing with possible MM signal changes under pathological conditions. The MM spectrum becomes more structured at increased magnetic field strengths and the estimation of MM contributions by smooth mathematical functions is not able to completely describe all the features of the *in vivo* spectrum, especially in the 2–4 ppm range [58]. Therefore, including the experimentally measured MM spectrum in the basis set (as an extended prior knowledge) minimizes the bias and improves the reliability of metabolite quantification. Including the MM spectrum in the basis set is most important for the quantification of weakly represented metabolites, such as Asc, GABA or GSH.

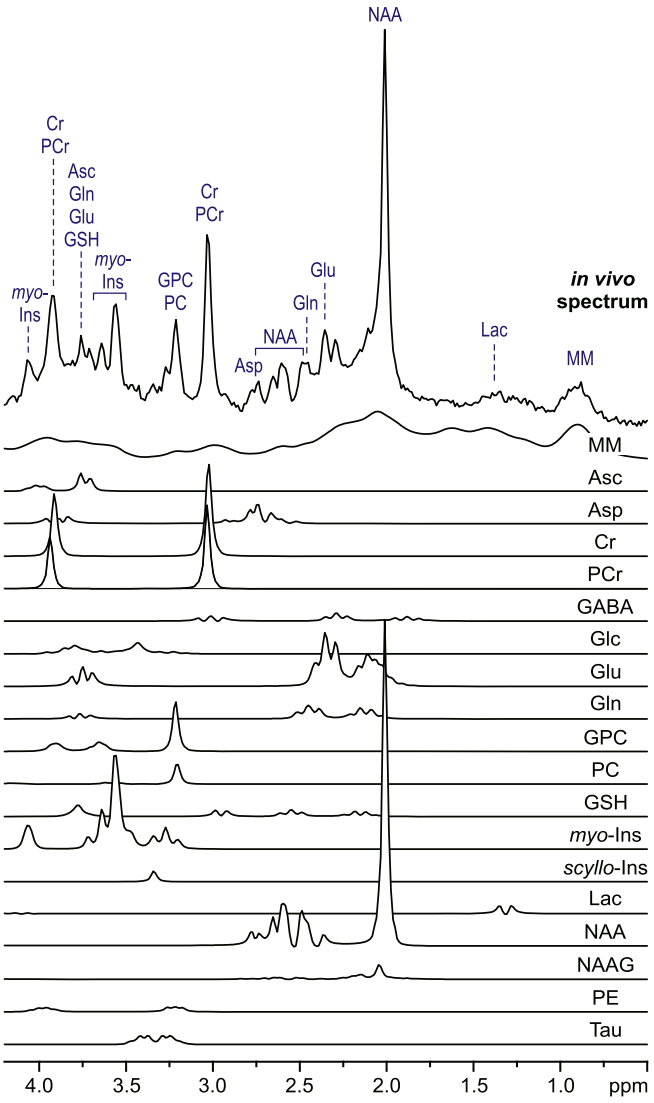

Fig. 7. The LCModel analysis of an *in vivo* ^{1}H MR spectrum acquired from a human brain at 3 T (semi-LASER, TE = 28 ms, TR = 5 s, NT = 160, VOI = 8 ml, gray-matter-rich occipital cortex). Courtesy of Dr. Petr Bednařík from the University of Minnesota.

Concentration references

The methyl signal of total creatine (tCr) at 3.03 ppm has been widely used as an internal concentration references. However, tCr concentration changes across brain regions and could be altered under different pathophysiological conditions. A much more robust approach for the scaling of estimated metabolite concentrations from short echo-time spectra is to use the unsuppressed water signal as an internal reference, which requires knowledge of the brain's tissue composition and water content within the selected VOI. In order to avoid underestimation of metabolite concentrations, the signal contribution from the cerebrospinal fluid must be eliminated using the differences in T_2 relaxation (multiple TE approach) or utilizing MRI based segmentation methods. The best approach currently available for absolute metabolite quantification is to use a long TR and ultra-short TE, which reduces relaxation effects to the level that corrections are not necessary. An alternate choice is to use an external phantom that contains a solution with known metabolite concentrations. The phantom should be placed in the same position as the subject with matched RF coil loading to mimic *in vivo* experimental conditions. However, this approach is

difficult at high magnetic fields because of the increased spatial inhomogeneity of transmit the B_1^+ field. The ERETIC (Electronic REference To access In vivo Concentrations) method, which generates an artificial signal using an external RF generator or additional RF channel, has been used to determine absolution concentrations in high-resolution NMR spectroscopy of liquids [65]. Recently this method has been extended to *in vivo* MRS and showed results consistent with those obtained using a water reference in healthy volunteers [66]. Like external phantom referencing, correction for the B_1 field spatial inhomogeneity must be taken into account. Overall, unsuppressed water signal as an internal reference is preferentially used because it is not only very simple, but it provides highly robust metabolite quantification.

Neurochemical profiling

Advanced *in vivo* ^{1}H-MRS is capable of providing information on an extended range of brain metabolites with higher precision and accuracy. These features substantially increase the importance and value of ^{1}H-MRS in neuroscience research. The non-invasive nature of ^{1}H-MRS makes the method ideal for longitudinal studies of mouse and rat models of human diseases [19,23]. There are not too many high-field neurochemical profiling studies in the human brain to date [5,9,32,42,67]. These studies demonstrate that neurochemical profiling is feasible in humans and the precision of metabolite quantification has become high enough to detect inter-individual differences in metabolite levels. These methods are sensitive enough to detect neurochemical changes induced by brain activation [14–17,68]. Fortunately, advanced ^{1}H-MRS techniques developed for humans at ultra-high fields can substantially improve the performance of ^{1}H-MRS on 3T clinical MR scanners (Fig. 7) [69,70], which opens an opportunity for routine neurochemical profiling on patients.

References

[1] J. Pfeuffer, I. Tkac, S.W. Provencher, R. Gruetter, Toward an in vivo neurochemical profile: quantification of 18 metabolites in short-echo-time (1)H NMR spectra of the rat brain, J. Magn. Reson. 141 (1999) 104–120.

[2] I. Tkac, P. Andersen, G. Adriany, H. Merkle, K. Ugurbil, R. Gruetter, In vivo 1H NMR spectroscopy of the human brain at 7 T, Magn. Reson. Med. 46 (2001) 451–456.

[3] I. Tkac, R. Gruetter, Methodology of H NMR spectroscopy of the human brain at very high magnetic fields, Appl. Magn. Reson. 29 (2005) 139–157.

[4] I. Tkac, P.G. Henry, P. Andersen, C.D. Keene, W.C. Low, R. Gruetter, Highly resolved in vivo 1H NMR spectroscopy of the mouse brain at 9.4 T, Magn. Reson. Med. 52 (2004) 478–484.

[5] R. Mekle, V. Mlynarik, G. Gambarota, M. Hergt, G. Krueger, R. Gruetter, MR spectroscopy of the human brain with enhanced signal intensity at ultrashort echo times on a clinical platform at 3T and 7T, Magn. Reson. Med. 61 (2009) 1279–1285.

[6] M. Terpstra, I. Cheong, T. Lyu, D.K. Deelchand, U.E. Emir, P. Bednarik, L.E. Eberly, G. Oz, Test-retest reproducibility of neurochemical profiles with short-echo, single-voxel MR spectroscopy at 3T and 7T, Magn. Reson. Med. 76 (2016) 1083–1091.

[7] G. Gambarota, L. Xin, C. Perazzolo, I. Kohler, V. Mlynarik, R. Gruetter, In vivo 1H NMR measurement of glycine in rat brain at 9.4 T at short echo time, Magn. Reson. Med. 60 (2008) 727–731.

[8] M. Terpstra, K. Ugurbil, I. Tkac, Noninvasive quantification of human brain ascorbate concentration using 1H NMR spectroscopy at 7 T, NMR Biomed. 23 (2010) 227–232.

[9] I. Tkac, G. Oz, G. Adriany, K. Ugurbil, R. Gruetter, In vivo 1H NMR spectroscopy of the human brain at high magnetic fields: metabolite quantification at 4T vs. 7T, Magn. Reson. Med. 62 (2009) 868–879.

[10] I. Tkac, Z. Starcuk, I.Y. Choi, R. Gruetter, In vivo 1H NMR spectroscopy of rat brain at 1 ms echo time, Magn. Reson. Med. 41 (1999) 649–656.

[11] V. Mlynarik, C. Cudalbu, L. Xin, R. Gruetter, 1H NMR spectroscopy of rat brain in vivo at 14.1Tesla: improvements in quantification of the neurochemical profile, J. Magn. Reson. 194 (2008) 163–168.

[12] D.K. Deelchand, P.F. Van de Moortele, G. Adriany, I. Iltis, P. Andersen, J.P. Strupp, J.T. Vaughan, K. Ugurbil, P.G. Henry, In vivo 1H NMR spectroscopy of the human brain at 9.4 T: initial results, J. Magn. Reson. 206 (2010) 74–80.

[13] S.T. Hong, D.Z. Balla, G. Shajan, C. Choi, K. Ugurbil, R. Pohmann, Enhanced neurochemical profile of the rat brain using in vivo (1)H NMR spectroscopy at 16.4 T, Magn. Reson. Med. 65 (2011) 28–34.

[14] Y. Lin, M.C. Stephenson, L. Xin, A. Napolitano, P.G. Morris, Investigating the metabolic changes due to visual stimulation using functional proton magnetic resonance spectroscopy at 7 T, J. Cereb. Blood Flow. Metab. 32 (2012) 1484–1495.

[15] S. Mangia, I. Tkac, R. Gruetter, P.F. Van de Moortele, B. Maraviglia, K. Ugurbil, Sustained neuronal activation raises oxidative metabolism to a new steady-state level: evidence from 1H NMR spectroscopy in the human visual cortex, J. Cereb. Blood Flow. Metab. 27 (2007) 1055–1063.

[16] B. Schaller, R. Mekle, L. Xin, N. Kunz, R. Gruetter, Net increase of lactate and glutamate concentration in activated human visual cortex detected with magnetic resonance spectroscopy at 7 tesla, J. Neurosci. Res. 91 (2013) 1076–1083.

[17] B. Schaller, L. Xin, K. O'Brien, A.W. Magill, R. Gruetter, Are glutamate and lactate increases ubiquitous to physiological activation? A (1)H functional MR spectroscopy study during motor activation in human brain at 7Tesla, NeuroImage 93 (1) (2014) 138–145.

[18] A. Marsman, R.C. Mandl, D.W. Klomp, M.M. Bohlken, V.O. Boer, A. Andreychenko, W. Cahn, R.S. Kahn, P.R. Luijten, H.E. Hulshoff Pol, GABA and glutamate in schizophrenia: a 7 T (1)H-MRS study, NeuroImage Clin. 6 (2014) 398–407.

[19] J.M. das Neves Duarte, A. Kulak, M.M. Gholam-Razaee, M. Cuenod, R. Gruetter, K.Q. Do, N-acetylcysteine normalizes neurochemical changes in the glutathione-deficient schizophrenia mouse model during development, Biol. Psychiatry 71 (2012) 1006–1014.

[20] I. Tkac, J.M. Dubinsky, C.D. Keene, R. Gruetter, W.C. Low, Neurochemical changes in Huntington R6/2 mouse striatum detected by in vivo 1H NMR spectroscopy, J. Neurochem. 100 (2007) 1397–1406.

[21] C. Berthet, H. Lei, J. Thevenet, R. Gruetter, P.J. Magistretti, L. Hirt, Neuroprotective role of lactate after cerebral ischemia, J. Cereb. Blood Flow. Metab. 29 (2009) 1780–1789.

[22] V. Mlynarik, M. Cacquevel, L. Sun-Reimer, S. Janssens, C. Cudalbu, H. Lei, B.L. Schneider, P. Aebischer, R. Gruetter, Proton and phosphorus magnetic resonance spectroscopy of a mouse model of Alzheimer's disease, J. Alzheimer's Dis. : JAD 31 (Suppl 3) (2012) S87–S99.

[23] G. Oz, C.D. Nelson, D.M. Koski, P.G. Henry, M. Marjanska, D.K. Deelchand, R. Shanley, L.E. Eberly, H.T. Orr, H.B. Clark, Noninvasive detection of presymptomatic and progressive neurodegeneration in a mouse model of spinocerebellar ataxia type 1, J. Neurosci. 30 (2010) 3831–3838.

[24] P.F. Van de Moortele, C. Akgun, G. Adriany, S. Moeller, J. Ritter, C.M. Collins, M.B. Smith, J.T. Vaughan, K. Ugurbil, B(1) destructive interferences and spatial phase patterns at 7 T with a head transceiver array coil, Magn. Reson. Med. 54 (2005) 1503–1518.

[25] G.J. Metzger, C. Snyder, C. Akgun, T. Vaughan, K. Ugurbil, P.F. Van de Moortele, Local B1+ shimming for prostate imaging with transceiver arrays at 7T based on subject-dependent transmit phase measurements, Magn. Reson. Med. 59 (2008) 396–409.

[26] T. Vaughan, L. DelaBarre, C. Snyder, J. Tian, C. Akgun, D. Shrivastava, W. Liu, C. Olson, G. Adriany, J. Strupp, P. Andersen, A. Gopinath, P.F. van de Moortele, M. Garwood, K. Ugurbil, 9.4T human MRI: preliminary results, Magn. Reson. Med. 56 (2006) 1274–1282.

[27] U. Katscher, P. Bornert, C. Leussler, J.S. van den Brink, Transmit SENSE, Magn. Reson. Med. 49 (2003) 144–150.

[28] S. Saekho, C.Y. Yip, D.C. Noll, F.E. Boada, V.A. Stenger, Fast-kz three-dimensional tailored radiofrequency pulse for reduced B1 inhomogeneity, Magn. Reson. Med. 55 (2006) 719–724.

[29] K. Setsompop, V. Alagappan, B.A. Gagoski, A. Potthast, F. Hebrank, U. Fontius, F. Schmitt, L.L. Wald, E. Adalsteinsson, Broadband slab selection with B1+ mitigation at 7T via parallel spectral-spatial excitation, Magn. Reson. Med. 61 (2009) 493–500.

[30] J.E. Snaar, W.M. Teeuwisse, M.J. Versluis, M.A. van Buchem, H.E. Kan, N.B. Smith, A.G. Webb, Improvements in high-field localized MRS of the medial temporal lobe in humans using new deformable high-dielectric materials, NMR Biomed. 24 (2011) 873–879.

[31] W.M. Teeuwisse, W.M. Brink, K.N. Haines, A.G. Webb, Simulations of high permittivity materials for 7 T neuroimaging and evaluation of a new barium titanate-based dielectric, Magn. Reson. Med. 67 (2012) 912–918.

[32] U.E. Emir, E.J. Auerbach, P.F. Moortele, M. Marjanska, K. Ugurbil, M. Terpstra, I. Tkac, G. Oz, Regional neurochemical profiles in the human brain measured by (1) H MRS at 7 T using local B(1) shimming, NMR Biomed. 25 (2011) 152–160.

[33] R.A. de Graaf, In Vivo NMR Spectroscopy – 2nd Edition: Principles and Techniques, John Wiley & Sons, Ltd, 2007.

[34] R. Gruetter, Automatic, localized in vivo adjustment of all first- and second-order shim coils, Magn. Reson. Med. 29 (1993) 804–811.

[35] R. Gruetter, I. Tkac, Field mapping without reference scan using asymmetric echo-planar techniques, Magn. Reson. Med. 43 (2000) 319–323.

[36] J. Shen, R.E. Rycyna, D.L. Rothman, Improvements on an in vivo automatic shimming method [FASTERMAP], Magn. Reson. Med. 38 (1997) 834–839.

[37] A. Haase, J. Frahm, W. Hanicke, D. Matthaei, 1H NMR chemical shift selective (CHESS) imaging, Phys. Med. Biol. 30 (1985) 341–344.

[38] R.J. Ogg, P.B. Kingsley, J.S. Taylor, WET, a T1- and B1-insensitive water-suppression method for in vivo localized 1H NMR spectroscopy, J. Magn. Reson. B 104 (1994) 1–10.

[39] V. Mlynarik, G. Gambarota, H. Frenkel, R. Gruetter, Localized short-echo-time

proton MR spectroscopy with full signal-intensity acquisition, Magn. Reson. Med. 56 (2006) 965–970.
[40] L. Xin, B. Schaller, V. Mlynarik, H. Lu, R. Gruetter, Proton T1 relaxation times of metabolites in human occipital white and gray matter at 7 T, Magn. Reson. Med. 69 (2013) 931–936.
[41] T.W. Scheenen, D.W. Klomp, J.P. Wijnen, A. Heerschap, Short echo time 1H-MRSI of the human brain at 3T with minimal chemical shift displacement errors using adiabatic refocusing pulses, Magn. Reson. Med. 59 (2008) 1–6.
[42] G. Oz, I. Tkac, Short-echo, single-shot, full-intensity proton magnetic resonance spectroscopy for neurochemical profiling at 4 T: validation in the cerebellum and brainstem, Magn. Reson. Med. 65 (2011) 901–910.
[43] A. Haase, Localization of unaffected spins in NMR imaging and spectroscopy (LOCUS spectroscopy), Magn. Reson. Med. 3 (1986) 963–969.
[44] J.H. Duyn, J. Gillen, G. Sobering, P.C. van Zijl, C.T. Moonen, Multisection proton MR spectroscopic imaging of the brain, Radiology 188 (1993) 277–282.
[45] J. Frahm, K.-D. Merboldt, W. Hanicke, Localized proton spectroscopy using stimulated echoes, J. Magn. Reson. 72 (1987) (1969) 502–508.
[46] R.J. Ordidge, A. Connelly, J.A.B. Lohman, Image-selected in Vivo spectroscopy (ISIS). A new technique for spatially selective NMR spectroscopy, J. Magn. Reson. 66 (1986) (1969) 283–294.
[47] A. Tannus, M. Garwood, Adiabatic pulses, NMR Biomed. 10 (1997) 423–434.
[48] M. Garwood, L. DelaBarre, The return of the frequency sweep: designing adiabatic pulses for contemporary NMR, J. Magn. Reson. 153 (2001) 155–177.
[49] N. Allaili, R. Valabregue, E.J. Auerbach, V. Guillemot, L. Yahia-Cherif, E. Bardinet, M. Jabourian, P. Fossati, S. Lehericy, M. Marjanska, Single-voxel (1) H spectroscopy in the human hippocampus at 3 T using the LASER sequence: characterization of neurochemical profile and reproducibility, NMR Biomed. 28 (2015) 1209–1217.
[50] K. Ennis, D.K. Deelchand, I. Tkac, P.G. Henry, R. Rao, Determination of oxidative glucose metabolism in vivo in the young rat brain using localized direct-detected (1)(3)C NMR spectroscopy, Neurochem. Res. 36 (2011) 1962–1968.
[51] U. Klose, In vivo proton spectroscopy in presence of eddy currents, Magn. Reson. Med. 14 (1990) 26–30.
[52] S.W. Provencher, Estimation of metabolite concentrations from localized in vivo proton NMR spectra, Magn. Reson. Med. 30 (1993) 672–679.
[53] H. Ratiney, M. Sdika, Y. Coenradie, S. Cavassila, D. van Ormondt, D. Graveron-Demilly, Time-domain semi-parametric estimation based on a metabolite basis set, NMR Biomed. 18 (2005) 1–13.
[54] M. Wilson, G. Reynolds, R.A. Kauppinen, T.N. Arvanitis, A.C. Peet, A constrained least-squares approach to the automated quantitation of in vivo (1)H magnetic resonance spectroscopy data, Magn. Reson. Med. 65 (2011) 1–12.
[55] V. Govindaraju, K. Young, A.A. Maudsley, Proton NMR chemical shifts and coupling constants for brain metabolites, NMR Biomed. 13 (2000) 129–153.
[56] G. Helms, The principles of quantification applied to in vivo proton MR spectroscopy, Eur. J. Radiol. 67 (2008) 218–229.
[57] S. Provencher, LCModel & LCMgui User's Manual, 2013.
[58] C. Cudalbu, V. Mlynarik, L.J. Xin, R. Gruetter, Comparison of two approaches to model the macromolecule spectrum for the quantification of short TE (1)H MRS spectra, I W Imag. Syst. Tech. (2008) 309–312.
[59] K.L. Behar, T. Ogino, Characterization of macromolecule resonances in the 1H NMR spectrum of rat brain, Magn. Reson. Med. 30 (1993) 38–44.
[60] K.L. Behar, D.L. Rothman, D.D. Spencer, O.A. Petroff, Analysis of macromolecule resonances in 1H NMR spectra of human brain, Magn. Reson. Med. 32 (1994) 294–302.
[61] N. Kunz, C. Cudalbu, V. Mlynarik, P.S. Huppi, S.V. Sizonenko, R. Gruetter, Diffusion-weighted spectroscopy: a novel approach to determine macromolecule resonances in short-echo time 1H-MRS, Magn. Reson. Med. 64 (2010) 939–946.
[62] J.B. Poullet, D.M. Sima, A.W. Simonetti, B. De Neuter, L. Vanhamme, P. Lemmerling, S. Van Huffel, An automated quantitation of short echo time MRS spectra in an open source software environment: AQSES, NMR Biomed. 20 (2007) 493–504.
[63] B. Schaller, L. Xin, C. Cudalbu, R. Gruetter, Quantification of the neurochemical profile using simulated macromolecule resonances at 3 T, NMR Biomed. 26 (2013) 593–599.
[64] B. Schaller, L. Xin, R. Gruetter, Is the macromolecule signal tissue-specific in healthy human brain? A H MRS study at 7 tesla in the occipital lobe, Magn. Reson. Med. 72 (2014) 934–940.
[65] S. Akoka, L. Barantin, M. Trierweiler, Concentration measurement by proton NMR using the ERETIC method, Anal. Chem. 71 (1999) 2554–2557.
[66] H. Desal, N. Pineda Alonso, S. Akoka, Electronic reference for absolute quantification of brain metabolites by 1H-MRS on clinical whole-body imaging, J. Neuroradiol. J. de Neuroradiol. 37 (2010) 292–297.
[67] B.L. van de Bank, U.E. Emir, V.O. Boer, J.J. van Asten, M.C. Maas, J.P. Wijnen, H.E. Kan, G. Oz, D.W. Klomp, T.W. Scheenen, Multi-center reproducibility of neurochemical profiles in the human brain at 7 T, NMR Biomed. 28 (2015) 306–316.
[68] P. Bednarik, I. Tkac, F. Giove, M. DiNuzzo, D.K. Deelchand, U.E. Emir, L.E. Eberly, S. Mangia, Neurochemical and BOLD responses during neuronal activation measured in the human visual cortex at 7 Tesla, J. Cereb. Blood Flow. Metab. 35 (2015) 601–610.
[69] P. Bednarik, A. Moheet, D.K. Deelchand, U.E. Emir, L.E. Eberly, M. Bares, E.R. Seaquist, G. Oz, Feasibility and reproducibility of neurochemical profile quantification in the human hippocampus at 3 T, NMR Biomed. 28 (2015) 685–693.
[70] D.K. Deelchand, I.M. Adanyeguh, U.E. Emir, T.M. Nguyen, R. Valabregue, P.G. Henry, F. Mochel, G. Oz, Two-site reproducibility of cerebellar and brainstem neurochemical profiles with short-echo, single-voxel MRS at 3T, Magn. Reson. Med. 73 (2015) 1718–1725.
[71] F. Eggenschwiler, T. Kober, A.W. Magill, R. Gruetter, J.P. Marques, SA2RAGE: a new sequence for fast B1+ -mapping, Magn. Reson. Med. 67 (2012) 1609–1619.
[72] J. McKay, I. Tkac, Quantitative in vivo neurochemical profiling in humans: where are we now? Int. J. Epidemiol. 45 (5) (2016) in press.